Int. J. Electrochem. Sci., 13 **(2018)** 8094 – 8107, doi: 10.20964/2018.08.52

International Journal of
ELECTROCHEMICAL
SCIENCE
www.electrochemsci.org

Short Communication

Effects of sodium lignosulfonate on bismuth electrochemical deposition on copper surfaces from HCl-NaCl-$BiCl_3$ solution

Yun-long HE [1], *Rui-dong XU*[1,2,*], *Shi-wei HE*[1], *Han-sen CHEN*[1], *Kuo Li*[1], *Yun ZHU*[1], *Qing-feng SHEN*[1]

[1] Faculty of Metallurgical and Energy Engineering, Kunming University of Science and Technology, Kunming 650093, China;
[2] State Key Laboratory of Complex Nonferrous Metal Resources Clean Utilization, Kunming 650093, China
[*]E-mail: rdxupaper@aliyun.com

Received: 23 April 2018 / *Accepted:* 31 May 2018 / *Published:* 5 July 2018

The effects of sodium lignosulfonate (SLS) on bismuth electrochemical deposition on copper surfaces from HCl-NaCl-$BiCl_3$ solution were investigated. Cyclic voltammetry studies indicated that the Bi^{3+} ions could be reduced electrolytically to bismuth on the surface of copper in the presence of different concentrations of SLS and that 0.3 g/L of SLS was beneficial for the electroreduction of Bi^{3+}. The cathodic polarization study indicated that SLS had a noticeable effect on the Tafel slope and exchange current density but no significant effect on the transfer coefficients. SEM images revealed that the deposit grain size decrease remarkably when sodium lignosulfonate was added to the electrolytic bath and that the main textures of the deposits changed from a blocky structure to a lamellar structure when the sodium lignosulfonate concentration increased from 0.1 to 0.4 g/L. XRD analysis indicated that the addition of sodium lignosulfonate could slightly suppress the (110) orientation and enhance the other crystallographic orientations significantly and that the most significantly enhanced crystallographic orientation was the (104) plane.

Keywords: sodium lignosulfonate, bismuth, deposit morphology, crystallographic orientation

1. INTRODUCTION

In recent years, bismuth has received considerable attention due to its wide application in various areas based on its outstanding physicochemical and electrical properties. Bismuth is an important semimetal that has unusual electrical, physical and chemical properties, such as a low carrier concentration, highly anisotropic Fermi surface, and long carrier mean free path [1]. Many bismuth materials, such as Bi single crystals [2], thin films [3,4], and nanowires [5,6] have demonstrated high magnetoresistance effects; therefore, bismuth can be considered a promising candidate material for magnetic sensors. Additionally, bismuth film electrodes (BFEs) have been adopted to detect metallic ions and organic compounds [2, 7]. Because of its other outstanding characteristics, bismuth has also been used as a corrosion-protective interlayer in battery electrodes [8] and decorative coatings. Bismuth is utilized as a decorative coating mainly because this kind of coating provides excellent inhibition of hydrogen embitterment. On the other hand, bismuth has been demonstrated to be a low-toxicity and environmentally friendly metal, and naturally, bismuth can be extensively used as a pharmaceutical material [1].

Based on the advantages of the wide applications of bismuth, pure metallic bismuth as a basic material plays a fundamental role in the various applications of this element. Hence, it is of great significance to investigate the preparation process of pure bismuth. It is known that most of the important nonferrous metals, such as zinc, copper and nickel, are commercially produced using aqueous electrochemical deposition processes [10]. Similarly, the electrochemical deposition process provides a simple route to prepare pure bismuth due to its remarkable advantages, such as a high deposition rate, use in mass production, and successful industrial applications.

Although the properties of the metal layer, including the electrolyte concentration, complexants, pH, and temperature, as well as the current density and potential, are highly influenced by the electrodeposition bath [11,13], generally, electrolytic operations are sensitive to the addition of both inorganic and organic impurities[14]. The metal deposit quality, energy consumption, crystal size, and morphology can be drastically affected when inorganic or organic impurities are present in appreciable concentrations in the electrolyte. In investigating the effect mechanism of organic impurities, the influence of organic additives on the deposition of metals from electrodeposition baths has become an interesting subject. Many organic impurities, such as gelatin, polyethylene glycol (PEG), citric acid (CA) and ethylenediaminetetraacetic acid (EDTA), have been employed to systematically study their effects on the electrodeposition of bismuth. It has been reported that after adsorbing PEG onto Bi deposits, the adhesion of deposits was improved, while the formation of dendrites in the deposit was inhibited [7].

Lignosulfonates are widely used organic additives [15] that can be obtained as polyelectrolytes when wood or other plant raw materials are used for manufacturing cellulose by the sulfite method [16]. Due to the presence of sulfonic groups in their structure, lignosulfonates show ion-exchange and surface-active properties and have been applied in various industrial processes [17]; these compounds have been used as dispersing agents and set-retarding agents in the concrete admixture industry [18], adhesives [19], etc.

Sodium lignosulfonate (SLS) is a kind of water-soluble lignin sulfo-derivative that contains hydrophobic groups (carbon chains) and many hydrophilic radicals, such as phenylic hydroxyl, sulfonic, and alcoholic hydroxyl groups [17]. SLS can be used as a kind of anionic surfactant; it can promote surface adsorption, further particle dispersion, and form thin films on metal surfaces due to its surface activity. Owing to its cost-effectiveness, eco-friendliness and ease of application [20], sodium lignosulfonate (SLS) is a widely used additive in different industrial processes. It can be used as a brightener agent during the electrodeposition of nickel [21] and lead [22]. Additionally, it can be applied as a kind of anticoagulant during the selenium electrochemical deposition process [23]. It has recently been reported that SLS was used as an additive for the fabrication of $Bi_{0.5}Sb_{1.5}Te_3$ films [24] and Bi_2Te_3 films [25] and for the electrodeposition of CdSe nanofilms on FTO/glass [26].

In the present work, SLS was employed as an organic additive during the electrodeposition of bismuth on copper surfaces in HCl-NaCl-$BiCl_3$ solution. The influence of SLS on bismuth electrodeposition was studied through cyclic voltammetry (CV) and cathodic polarization. Based on the cathodic polarization curves, many kinetic parameters (i.e., exchange current density, Tafel slope, and transfer coefficient) were obtained to better understand the electrode reactions during the electrodeposition of bismuth from HCl-NaCl-$BiCl_3$ solution. The surface microtopography and crystallographic orientation of the deposits were characterized by scanning electron microscopy (SEM) and X-ray diffraction (XRD), respectively.

2. EXPERIMENTAL

Cyclic voltammetry and cathodic polarization were carried out in a three-electrode system using an electrochemical working station (PARSTAT2273). Pure copper (the content of copper exceeded 99.99%) sheets were employed as working electrodes. The pure copper was cut into 10 mm (length)×10 mm (width)×2 mm (thickness) sheets, and then the copper sheets were sequentially polished by using 600- to 2000-grit SiC paper. Every polished copper sheet was rinsed with anhydrous ethanol (AR) and then washed by double-distilled water. The effective contact area of the copper sheets was controlled at 100 mm^2. The unused surfaces of the copper sheets were well sealed by using an insulating paste layer. An inert graphite electrode and saturated calomel electrode (SCE) were adopted as the counter electrode and reference electrode, respectively. The distance between the reference electrode and working electrode was approximately equal to four times the Luggin capillary diameter. The Luggin capillary was filled with agar and potassium chloride and used to link the reference electrode and working electrode. Potentials in this paper are referenced to the SCE. To confirm experimental reproducibility, every electrochemical experiment for the same condition was carried out at least three times.

Analytical-grade $BiCl_3$ and NaCl and double-distilled water were used to prepare all the solutions used in the experiments. The solutions used for every experiment were freshly prepared. The concentrations of $BiCl_3$ and NaCl were controlled at 120 g/L and 80 g/L, respectively, and the concentration of added HCl was 0.78 M. Pure nitrogen gas was purged into the solutions for 15 min before each experiment. All the electrodeposition experiments were performed for 50 min at a fixed current density of 150 A m^{-2}. After electrodeposition, the working electrode was removed and washed thoroughly by distilled water and then dried in a vacuum drying oven. During all experiments, the temperature was controlled at ambient temperature (~25℃); SLS concentrations varied from 0.0 to 0.4 g/L. The crystallographic orientation and microstructure of bismuth deposits were investigated by XRD and SEM.

3. RESULTS AND DISCUSSION

3.1. Cyclic voltammograms

The cyclic voltammetric curves measured in HCl-NaCl-$BiCl_3$ solution with SLS concentrations varying from 0 to 0.4 g/L are shown in Figure 1. The curves started at a potential of 0.1 V, reversed at -0.6 V and terminated at 0.1 V with a scan rate of 50 mV/s. Each cathodic branch of the cyclic voltammetric curve was characterized by a well-defined peak marked C_I. Peak C_I can be assigned to the deposition reaction of free Bi^{3+} [27], implying that Bi^{3+} ions can be reduced electrolytically to metallic bismuth on the surface of copper with the addition of different concentrations of SLS in the electrodeposition bath.

It can be seen from Fig. 1 that a single current peak was found in the cathodic branch of cyclic voltammetric curves and no visible current peak was found in the anodic branch. This phenomenon is ascribed to the voltage range chosen for the current test. The curves started at a potential of 0.1 V and scanned in the negative direction, which can avoid the dissolution of copper in the electrodeposition bath [28]. As previously mentioned, the single cathodic peak was marked as C_I and assigned to the reduction of Bi^{3+} ions. The overall reaction can be simplified as follows [29]:

$$Bi^{3+}+3e^{-}=Bi^{0} \qquad (1)$$

As shown in Fig. 1, the cyclic voltammetric curves exhibited a similar shape whether SLS was present or absent in the electrodeposition bath. The obvious difference among the cyclic voltammetric curves was the cathodic peak current density.

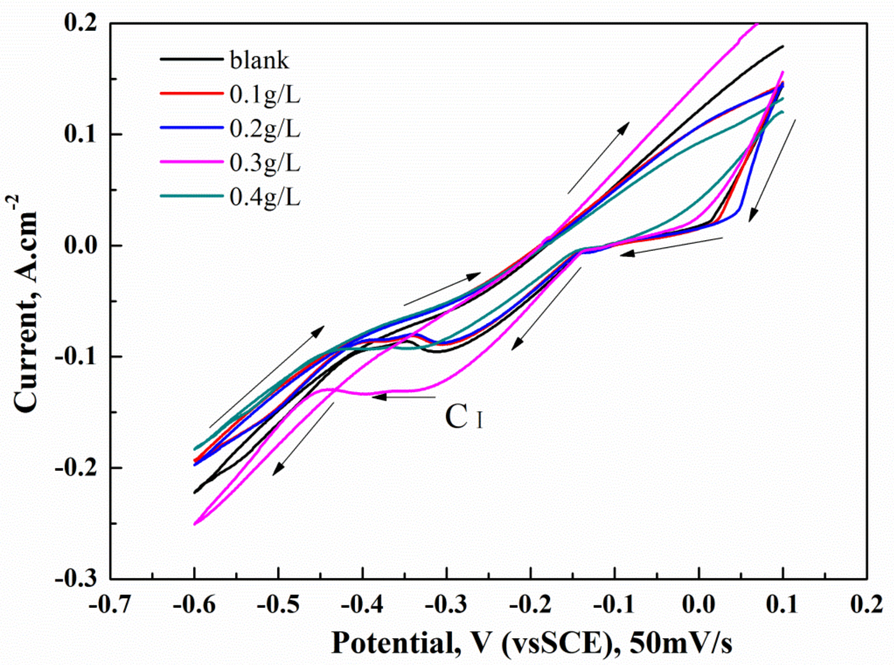

Figure 1. Cyclic voltammograms of copper electrodes in HCl-NaCl-$BiCl_3$ solutions with different sodium lignosulfonate (SLS) concentrations. The SLS concentration varied from 0.0 to 0.4 g/L (scan rate, 50 mV/s).

This phenomenon indicates that the concentration of SLS had an obvious effect on bismuth electrodeposition. It can be seen that the current density of peak C_I reached the maximum value when the concentration of SLS was controlled at 0.3 g/L, which indicates that the simultaneous addition of SLS is beneficial to the reduction of trivalent bismuth ions. On the other hand, the increase in the cathodic peak current density indicates that the electrochemical reaction can be improved. As previously mentioned, the main reaction that occurred on the surface was the reduction of Bi^{3+} ions; as shown in Equation (1), when the added concentration of SLS was fixed at 0.3 g/L, the reduction reaction could be enhanced.

However, when the added concentration of SLS was controlled at other levels, the cathodic peak current density decreased substantially, implying that when SLS was added at other concentrations, the electroreduction of Bi^{3+} ions could be suppressed. This tendency can be generally attributed to the adsorption of SLS on the surface of the copper: the adsorption layer can decrease mass transfer and cause a blocking effect on the surface of copper during the process of bismuth electrodeposition [30,31].

3.2. Cathodic potentiodynamic polarization study

Potentiodynamic polarization is a very useful technique; based on this technique, kinetic parameters can be investigated, and the electrochemical behavior of the electrode can be studied in the process of electrodeposition. Cathodic polarization curves were obtained by polarization of the electrode from -0.06 to -0.16 V. The scanning rate was fixed at 5 mV/s. The results are shown in Fig. 2. Usually, the current density of bismuth is controlled at 100~150 A/m^2 in industrial applications [32], but in the present work, a wider current density range of 100~200 A/m^2 was chosen to determine the kinetic parameters, including the transfer coefficient, Tafel slope, and exchange current density. Plots of the overpotential vs. the logarithm of current density are exhibited in Fig. 3. The overpotential of the bismuth was calculated from the following equation [33, 10]:

$$\eta=\varepsilon_{measured}+0.245\text{V}-\varepsilon_{equilibrium} \qquad (2)$$

$$\varepsilon_{equilibrium}=\varepsilon^{\theta}+\frac{RT}{3F}\ln a_{Bi^{3+}}=0.3087V \qquad (3)$$

where 0.245 V is the SCE potential vs. the standard hydrogen electrode (SHE) [34]; ε^{θ} is the standard electrode potential of Bi/Bi^{3+}, which is equal to 0.317 V [35]; $\varepsilon_{equilibrium}$ and $\varepsilon_{measured}$ are the equilibrium and measured potentials of the electrode, respectively; R stands for the molar gas constant (equal to 8.314 J mol^{-1} K^{-1}); F stands for the Faraday constant (equal to 96500 C mol^{-1}); T is the thermodynamic temperature (K); and $a_{Bi^{3+}}$ is the activity of Bi^{3+} ions.

According to the cathodic potentiodynamic polarization curves shown in Fig. 2, the electrochemical kinetic parameters can be analyzed and calculated according to Tafel's equation as follows:

$$\eta=a+b\log i \qquad (4)$$

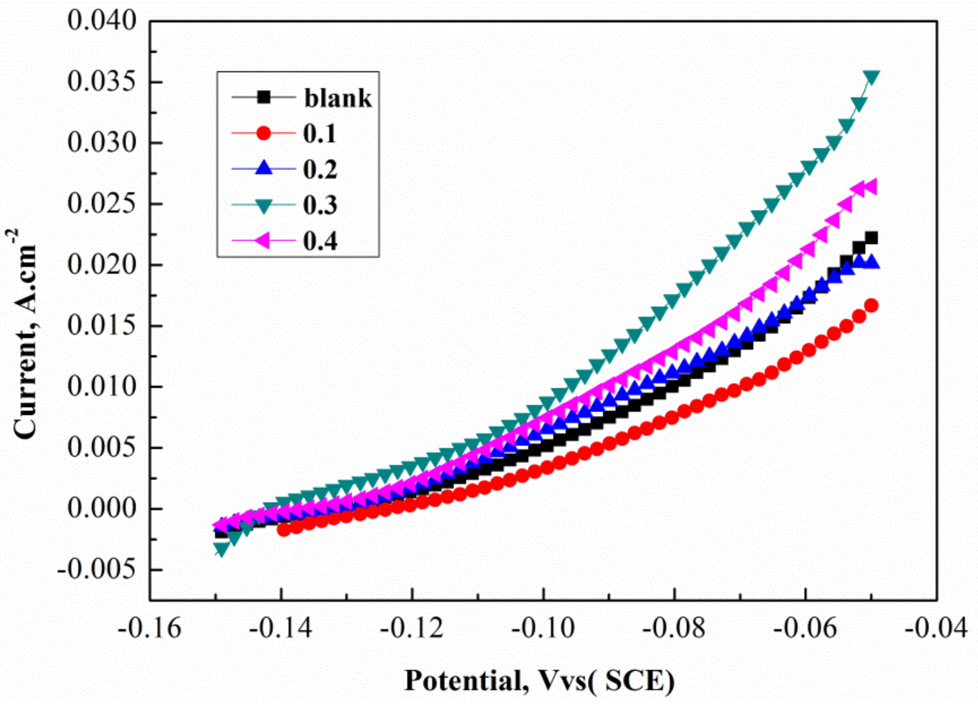

Figure 2. Effects of SLS concentration on cathodic polarization for bismuth electrodeposition from HCl-NaCl-$BiCl_3$ solution.

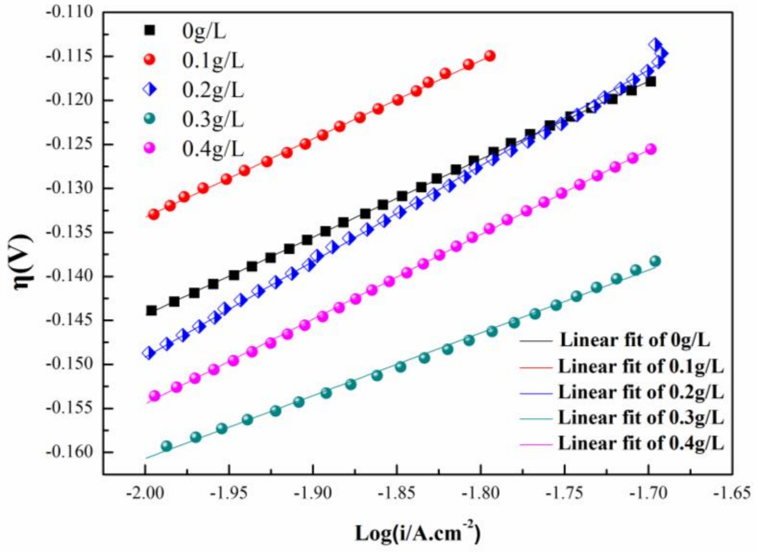

Figure 3. Plots of overpotential vs. the logarithm of current density for bismuth electrodeposition from HCl-NaCl-$BiCl_3$ solution

where η is the overpotential, a is the intercept and b is the Tafel slope. Based on the Butler-Volmer function, the function of the cathodic overpotential and current density of bismuth deposition on the copper surface can be written as follows[36]:

$$\eta = -\frac{2.303RT}{\alpha nF}\log i_0 + \frac{2.303RT}{\alpha nF}\log i \qquad (5)$$

where η is the overpotential, i_0 is the exchange current density and α is the charge-transfer coefficient of bismuth deposition. Compared with Equation (4) and Equation (5), the two following equations can be obtained:

$$a=-\frac{2.303RT}{\alpha nF}\log i_0 \qquad (6)$$

$$b=\frac{2.303RT}{\alpha nF} \qquad (7)$$

Table 1. Effects of SLS concentration on the cathodic kinetic parameters during bismuth electrodeposition from HCl-NaCl-$BiCl_3$ solution.

Concentration of SLS g/L	Tafel slope mV/dec	Exchange current density i_0 mA cm^{-2}	Transfer coefficient α
Blank	88	0.43	0.22
0.1	89	0.31	0.22
0.2	100	0.21	0.20
0.3	71	0.56	0.28
0.4	96	0.40	0.21

The cathodic kinetic parameters, such as the Tafel slope, b (mV decade^{-1}), transfer coefficient, α, and cathodic exchange current density, i_0 (mA cm^{-2}), for bismuth electrodeposition on copper electrodes are listed as a function of SLS concentration in Table 1. It was found that the Tafel slope was significantly influenced by the addition of SLS. It can be seen from Table 1 that the Tafel slope increased obviously when the SLS concentration increased from 0 to 0.1 g/L. With further addition of SLS, the Tafel slope increased substantially and reached the maximum value of 100 mV/decade when the SLS concentration was increased to 0.2 g/L. However, the Tafel slope decreased dramatically to the minimum value of 71 mV/decade when the SLS concentration was increased to 0.3 g/L. The decreased Tafel slopes observed on the copper electrode surface confirmed a depolarization effect [37] when the SLS concentration was 0.3 g/L. The main electrochemical reaction on the copper electrode surface was the electroreduction of Bi^{3+} (generation of metallic bismuth). Therefore, this depolarizing effect might be ascribed to the increased reduction rate of free trivalent bismuth ions. An appropriate concentration of SLS can improve the conditions for the electrodeposition of bismuth on the surface of copper, and hence, the electroreduction of Bi^{3+} can be accelerated.

This tendency was also confirmed by the variation in current density of peak C_I in the cyclic voltammogram exhibited in Fig. 1. It can be seen from Fig. 1 that the current density of peak C_I reached the maximum value when the SLS concentration was 0.3 g/L, implying that the SLS concentration of 0.3 g/L was beneficial to the electroreduction of Bi^{3+} in HCl-NaCl-$BiCl_3$ solution.

The effect of SLS concentration on the kinetic parameters for the electrodeposition of bismuth was also reflected in the exchange current density. A significant decrease in exchange current density was observed when the SLS concentration increased from 0 to 0.2 g/L. The decrease in i_0 was probably due to the decrease in active sites on the cathode surface [38], which indicates that the electron transfer rate of Bi^{3+} ions for electroreduction can be reduced. Usually, a decrease in active sites on the cathode surface is caused by the adsorption of the additive on the cathodic surface[39]. In the current study, when SLS was added in the range of 0~0.2 g/L, SLS could be adsorbed on the surface, leading to the blocking of active nucleation sites on the surface of the copper[31].

However, when the SLS concentration increased to 0.3 g/L, the exchange current density increased to the maximum value of 0.56 mA/cm^2. Generally, an increase in exchange current density implies that electrochemical reactions are accelerated [40]. Therefore, a high exchange current density usually indicates an increasing reaction rate [33]. Accordingly, the reaction rate of Bi^{3+} electrodeposition can be promoted on the surface of the copper; this speculation is in agreement with the results of the cyclic voltammetry curves (Fig. 1). On the other hand, the exchange current density increased substantially when the concentration of SLS was controlled at 0.3 g/L, which indicates that an appropriate concentration of SLS can improve the charge transfer and mass transfer reactions. It has been reported that, generally, charge transfer reactions determine the formation of the metallic film deposited at the interface between the cathode and the electrodeposition bath [41]. Therefore, the appropriate addition of SLS in the electrodeposition bath can significantly optimize the interface conditions. Better interface conditions between the cathode and the bath are beneficial to the electroreduction of Bi^{3+} ions.

It can be seen from Table 1 that the transfer coefficients changed only slightly with the addition of SLS during electrodeposition. This tendency indicates that the addition of SLS to HCl-NaCl-$BiCl_3$ solution did not significantly affect the transfer coefficients. The values of transfer coefficient α were essentially unaffected by the addition of SLS at almost all concentrations, indicating that the symmetry of the electron transfer reaction cannot be influenced during the electrodeposition of bismuth in HCl-NaCl-$BiCl_3$ solution [42-44].

3.2. Characterization of Deposits

To study the effect of SLS on the surface microtopography and crystallographic orientation of the electrodeposited bismuth, scanning electron microscopy (SEM) and X-ray diffraction (XRD) were employed. The surface morphology and crystallographic orientation were characterized by SEM and XRD, respectively. The surface microtopography and the XRD patterns of the bismuth deposits are given in Fig. 4 and Fig. 5, respectively.

It can be seen from Fig. 4b-e that SLS obviously influenced the morphology of the bismuth deposits compared with the morphology of the bismuth deposits obtained from electrodeposition without added SLS (Fig. 4a). The crystallite particle size decreased substantially when SLS addition increased from 0.0 to 0.1 g/L, and some tiny crystallites with varying sizes could be observed on the surfaces of the larger crystals. With the further addition of SLS up to 0.2 g/L, the morphology of the bismuth deposit changed to a lamellar structure consisting of random tiny crystallites. Increasing the SLS concentration from 0.3 g/L to 0.4 g/L resulted in a similar lamellar surface on the bismuth deposit. Moreover, the addition of SLS significantly increased the amount of tiny crystallites covering the lamellar surface. The addition of SLS led to more uniform and compact deposits with a further decrease in the size of the crystallites. Many randomly dispersed tiny crystallites appeared on the surface of the bismuth deposit, and the main textures of the deposits were changed from a blocky structure to a lamellar structure when SLS was used in the bath. The electrodeposits appear sufficiently well distributed and continuous.

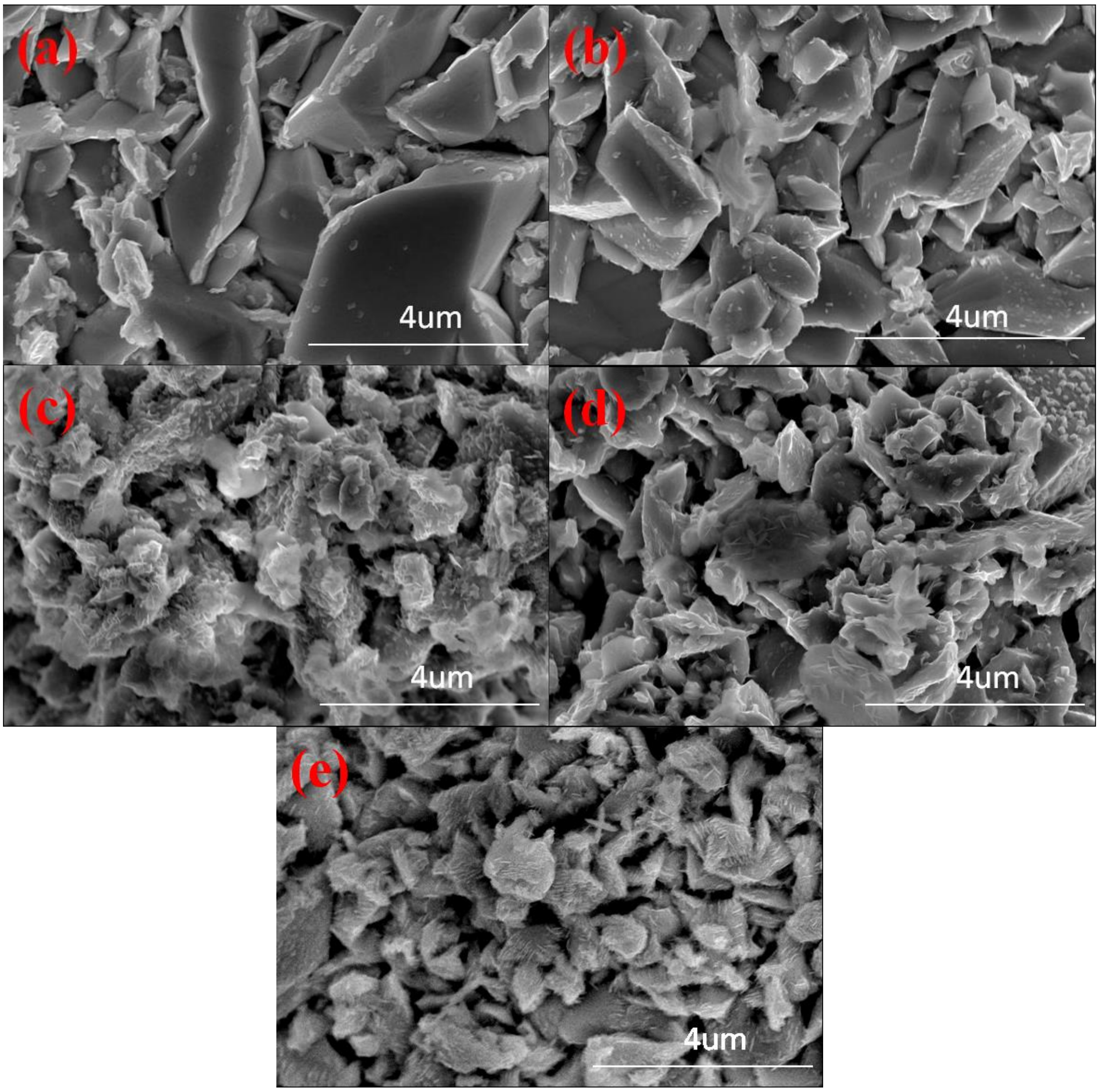

Figure 4. Scanning electron microscopy photomicrographs (×40000) of bismuth deposits obtained from different bath solutions with different added concentrations of SLS: (a) blank, (b) 0.1 g/L, (c) 0.2 g/L, (d) 0.3 g/L, and (e) 0.4 g/L.

This variation in morphology indicates that the surface of the bismuth deposits is strongly affected by the addition of SLS and that the microtopography of the bismuth deposit is very sensitive to the concentration of SLS used. When SLS is added to the electrodeposition bath, the organic additive can be absorbed on the surface of the copper sheet, which can change the surface properties. The addition of different concentrations of SLS will change the surface conditions and effectively change the crystal growth process of metallic bismuth. With increasing SLS concentration, the size of the crystallites was clearly decreased; this phenomenon was probably caused by specific adsorption and the mobility of SLS in the bath [45-46]. More absorbed SLS can provide more nucleation sites, and more different nucleation sites on the surface will cause the growth of deposits in many different places on the copper sheet and decrease the size of the crystallites.

The effect of SLS on the crystallographic orientation of electrodeposited bismuth was examined using X-ray diffraction. Figure 5a–e show the XRD patterns of bismuth films deposited from different baths with different added concentrations of SLS. The inherent crystal structure of bismuth is rhombohedral; this is slightly distorted from a cubic structure [47].

As seen from Fig. 5(a), the crystallographic orientation of bismuth deposited on the surface of copper can be noticeably influenced by the addition of SLS. The XRD patterns of bismuth deposits exhibited strong (012) and (110) peaks, while some other small peaks were also observed in the patterns, implying that the dominant crystal face was formed by crystallites in the (012) and (110) planes when SLS was absent from the plating bath. However, when SLS was added to the electrodeposition bath, the intensity of the (012) peak was noticeably enhanced, while the intensity of the (110) peak was suppressed markedly with the addition of SLS to the electrolyte solution. This tendency indicates that the addition of SLS is beneficial for obtaining good crystals in the (012) crystallographic orientation.

Moreover, an appreciable variation in crystallographic orientations can be observed from Fig. 5(b)-(c). It can be seen that the intensity of various peaks in different crystallographic orientations was significantly enhanced when SLS was used in the electrolysis system. It is interesting to note that with increased SLS, the intensity of the (104) orientation increased substantially compared with the intensity obtained for the sample without SLS, implying that the bismuth crystallites grew preferably in the direction of the (104) plane with the addition of SLS to the electrodeposition system. The intensity of various peaks in different crystal orientations was clearly pronounced with the addition of SLS. One possible explanation might be that the organic additive can be adsorbed on active sites, which is beneficial to the growth of the bismuth crystal in different crystallographic orientations [48].

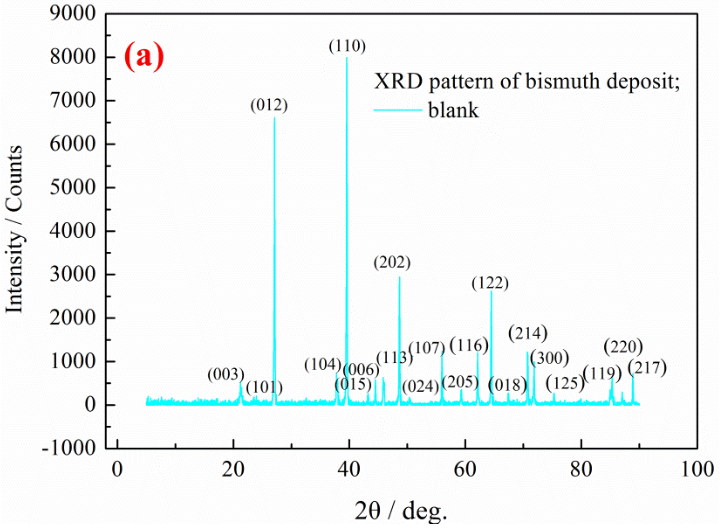

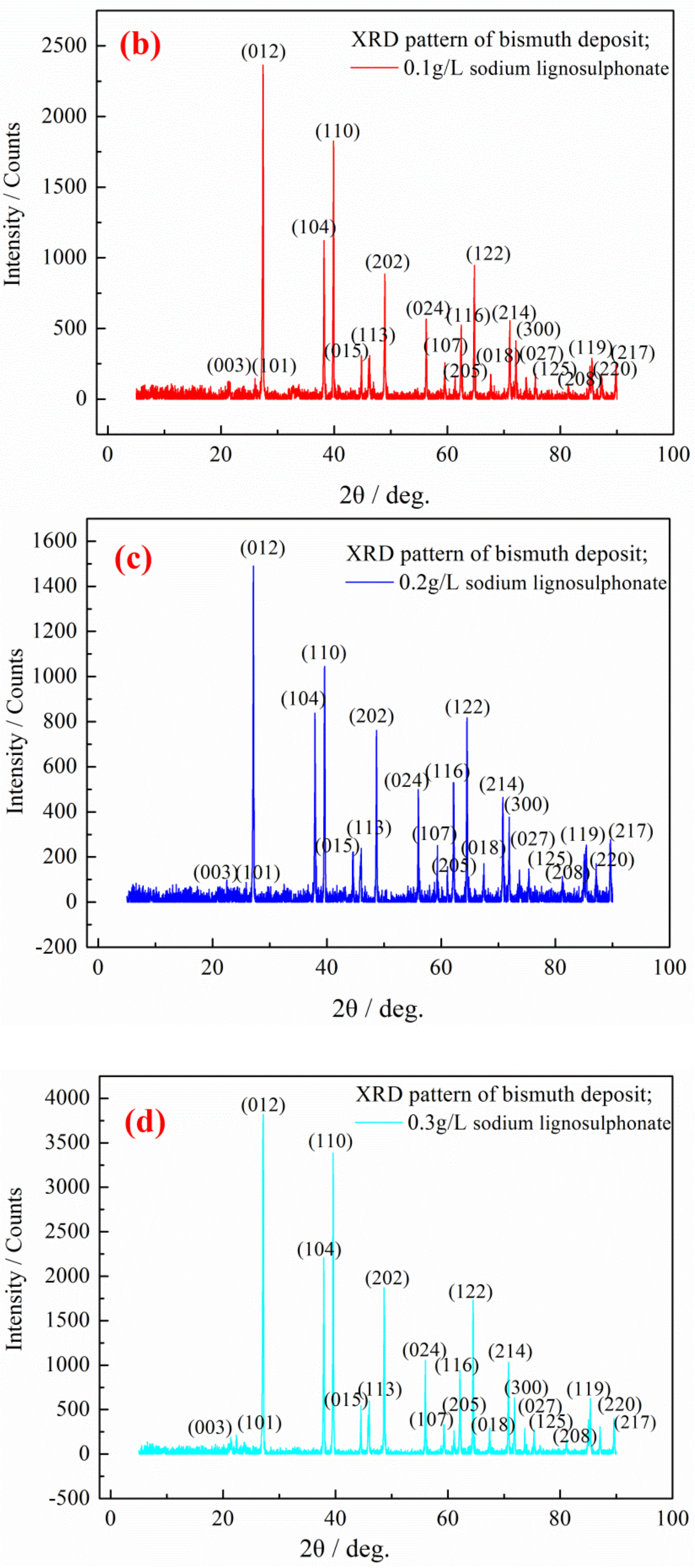
(b)
XRD pattern of bismuth deposit;
0.1g/L sodium lignosulphonate
Intensity / Counts
2θ / deg.
0
500
1000
1500
2000
2500
0
20
40
60
80
100
(012)
(110)
(104)
(202)
(122)
(024)
(116)
(214)
(300)
(113)
(015)
(107)
(205)
(018)
(027)
(125)
(208)
(119)
(217)
(220)
(003)
(101)
(c)
XRD pattern of bismuth deposit;
0.2g/L sodium lignosulphonate
Intensity / Counts
2θ / deg.
-200
0
200
400
600
800
1000
1200
1400
1600
0
20
40
60
80
100
(012)
(110)
(104)
(202)
(122)
(024)
(116)
(214)
(300)
(113)
(015)
(107)
(205)
(018)
(027)
(119)
(217)
(125)
(220)
(208)
(003)
(101)
(d)
XRD pattern of bismuth deposit;
0.3g/L sodium lignosulphonate
Intensity / Counts
2θ / deg.
-500
0
500
1000
1500
2000
2500
3000
3500
4000
0
20
40
60
80
100
(012)
(110)
(104)
(202)
(122)
(024)
(116)
(214)
(113)
(015)
(300)
(119)
(205)
(027)
(220)
(107)
(018)
(125)
(217)
(208)
(003)
(101)

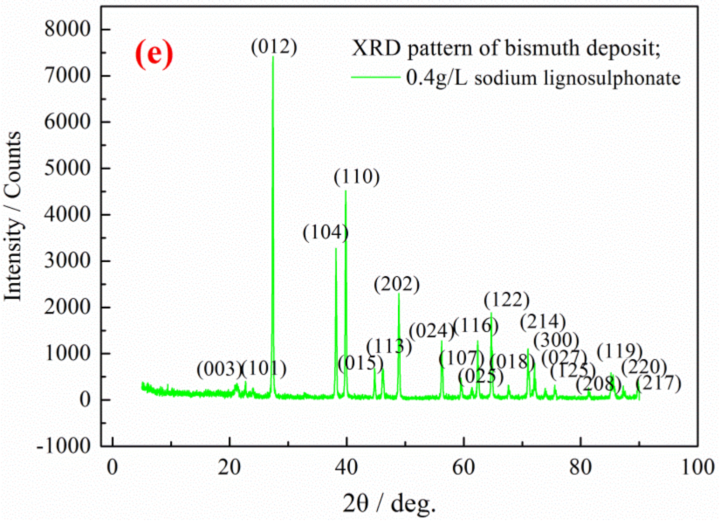

Figure 5. XRD patterns of bismuth deposits obtained from HCl-NaCl-$BiCl_3$ solution with different added concentrations of SLS: (a) blank, (b) 0.1 g/L, (c) 0.2 g/L, (d) 0.3 g/L, (e) 0.4 g/L.

In addition, the peak intensities of other various crystallographic orientations, such as (202), (015), (122), and (214), were obviously enhanced when the SLS concentration increased from 0.1 to 0.4 g/L in the electrolysis system. This variation indicates that the addition of SLS is beneficial to the growth of crystallite in various crystallographic orientations.

It should be mentioned here that although SLS is a widely used organic additive, the literature on bismuth electrodeposition with SLS as an additive has been very scarce until now. Therefore, it is worthwhile to present a simple comparison between the effects of other organic additives and SLS on bismuth electrodeposition.

Yi-Da Tsai et al.[7] have systematically investigated the effects of citric acid (CA), ethylenediaminetetraacetic acid (EDTA), polyethylene glycol (PEG), and gelatin on the deposition behavior of Bi. According to their research, PEG and gelatin could be adsorbed on the surface of Bi deposits, and SEM images indicated that PEG could improve the adhesion of the deposits and produce a smoother film. They also found that gelatin could form a compact shielding layer, which resulted in hydrogen evolution on the bismuth deposits. The evolution of hydrogen cracked the deposits and caused poor adhesion. The simultaneous use of PEG and gelatin could avoid the above defects and favor the formation of sphere-like Bi nanocrystals. The microstructure shape and crystal size could be controlled by varying the combination of CA, EDTA, PEG, and gelatin.

In the current investigation, the effects of SLS on the electrodeposition of bismuth on a surface copper electrode were studied. It can be concluded that the influence of SLS on the deposition of bismuth is quite different from the effects of CA, EDTA, PEG and gelatin on the electrodeposition of bismuth reported by the previous authors. Based on SEM analysis, the deposit grain size decreased remarkably when SLS was added to the electrolytic bath, and the main textures of the deposits were changed from a blocky structure to a lamellar structure with an increasing concentration of SLS. XRD analysis indicated that the (110) orientation could be slightly suppressed, while other crystallographic orientations could be enhanced significantly, and that the most significantly enhanced crystallographic orientation was the (104) plane.

4. CONCLUSION

(1) The cyclic voltammetry study indicated that the Bi^{3+} ions in HCl-NaCl-$BiCl_3$ solution could be reduced electrolytically to bismuth on the surface of copper in the presence of sodium lignosulfonate. A concentration of sodium lignosulfonate of 0.3 g/L was beneficial for the electroreduction of Bi^{3+}.

(2) The Tafel slope and exchange current density were significantly influenced by the addition of sodium lignosulfonate, while the addition of sodium lignosulfonate did not significantly affect the transfer coefficients, indicating that the symmetry of the electron transfer reaction cannot be influenced by the addition of SLS.

(3) According to surface morphology analysis, the crystallite particle size decreased substantially when sodium lignosulfonate was added to the electrolytic system. Random tiny crystallites appeared on the surface of the bismuth deposit, and the main textures of the deposits were changed from a blocky structure to a lamellar structure when the sodium lignosulfonate was increased from 0.1 to 0.4 g/L.

(4) XRD analysis indicated that the addition of sodium lignosulfonate could slightly suppress the (110) orientation and enhance the other crystallographic orientations significantly and that the most significantly enhanced crystallographic orientation was the (104) plane.

ACKNOWLEDGEMENTS
This work was financially supported by the National Natural Science Foundation of China (No. 51564031), an Independent Research Project of the State Key Laboratory of Complex Nonferrous Metal Resources Clean Utilization (No. CNMRCUTS1707), and the Cooperation between School and Enterprise of China (No. 0201352042) .

References

1. X.Y. Liu, P. Sun, S. Ren and L.S. Wen, *Electrochem. Commun.*, 10 (2008) 136.
2. E.A. Hutton, B. Ogorevc, S.B. Hočevar, F. Weldon, M.R. Smyth and J. Wang, *Electrochem. Commun.,* 12 (2001) 707.
3. F.Y. Yang, K. Liu, K. Hong, D.H. Reich, P.C. Searson and C.L. Chien, *Science,* 284 (1999) 1335.
4. Y. Kim, A.J. Freeman, G.K.L. Wong and J.B. Ketterson, *Appl. Phys. Lett*., 79 (2001) 3651.
5. S. Jiang, Y.H. Huang, F.Luo, N. Du and C.H. Yan, *Inorg. Chem. Commun.,* 6 (2003) 781.
6. R.A. Tolutis and S. Balevičius, *Phys. Status. Solidi.A.,* 203 (2010**)** 600.
7. Y.D. Tsai, C.H. Lien and C.C. Hu, *Electrochim. Acta,* 56 (2011) 7615.
8. F.Yang，K. Liu，C.L. Chen and P. Searson, *Phys. Rev. Lett.,* 82 (1999) 3328.
9. B. Popov, R. White and G. Zheng, *Corrosion,* 51 (1995) 429.
10. N. Sorour, W. Zhang, G. Gabra, E. Ghali and G. Houlach, *Hydrometallurgy,* 157 (2015) 261.
11. Y.D.Tsai, C.C. Hu and C.C. Lin, *Electrochim. Acta,* 53 (2007) 2040.
12. Y.D. Tsai and C.C. Hu, *J. Electrochem. Soc.*, 156 (2009) D58.
13. Y.D. Tsai and C.C. Hu, *J. Electrochem. Soc.,* 156 (2009) D490.
14. A.M. Alfantazi and D.B. Dreisinger, *Hydrometallurgy,* 69 (2003) 99.
15. G. Lotaa and G. Milczarek, *Electrochem. Commun.,* 13 (2011) 470.
16. G. Telysheva，T. Dizhbite， E. Paegle and A. Shapatin, *J. Appl. Polym. Sci.,* 82 (2001) 1013.

17. X.P.Ouyang, X.Q. Qiu, H.M. Lou and D.J. Yang, *Ind. Eng. Chem. Res.*, 45 (2006) 5716.
18. A. Macias and S. Goñi, *ACI Mater. J.*, 96 (1999) 40.
19. R.Chen and Q.Wu, *J. Appl. Polym. Sci.*, 52 (1994) 437.
20. Z. Dong, L. Wang and S. Zhao, *J. Arid Environ.*, 72 (2008) 1388.
21. L. Burgi, R.H. Friend and H. Sirringhaus, *Appl. Phys. Lett.*, 82 (2003) 1482.
22. K.P. Puntambekar, P.V. Pesavento and C.D. Frisbie, *Appl. Phys. Lett.*, 83 (2003) 5539.
23. J.R. Vig and J. W.LeBus, *IEEE Trans. on Parts Hyb. and Pack*,12 (1976) 365.
24. J. Kuleshova, E. Koukharenko, X. Li, N. Frety, I.S. Nandhakumar, J. Tudor, S.P. Beeby and N.M. White, *Langmuir*, 26 **(**2010**)** 16980.
25. O.C. Calero, P.D. Chao, B. Abad, C.V. Manzano, M.D. Ynsa, J.J. Romero, M.M. Rojo and M.S. M.González, *Electrochim. Acta***,** 123 (2014) 117.
26. M.B. Dergacheva, D. S.Puzikova, G.M. Khussurova, R.R. Nemkaeva and K.A. Mit, *Mater. Today***,** 4 (2017) 4572.
27. M.S. M. Gonzáez, A.L. Prieto and R. Gronsky, *J. Electrochem. Soc.*, 149 (2002) C546.
28. C. Agapescu, A. Cojocaru, A. Cotarta and Teodor Visan, *J. Appl. Electrochem.*, 43 (2013).309.
29. J. Schoenleber, N. Stein and C. Boulanger, *J. Electroanal. Chem.*, 724 (2014) 111.
30. B.C. Tripathy, S.C. Das, P. Singh, G.T. Hefter and V.N. Misra, *J. Appl. Electrochem.*, 565 (2004) 49.
31. Q.B. Zhang and Y.X. Hua, *J. Appl. Electrochem.*, 39 (2009) 261.
32. B.J.Chen and Z.D.Niu, *Design handbook for heavy nonferrous metal smelting: fascicule of lead, antimony, and bismuth*, Metallurgy Industry Press, Beijing, China**,** p. 663 (1995) [in Chinese].
33. N.Sorour, C.Su, E.Ghali and G.Houlachi, *Electrochim. Acta*, 258 (2017) 631.
34. S. W. Qiu, L. Li, H. Wang and Y. Wang, *J Electrochem. Soc.*, 164 (2017) E123.
35. G. James Speight, *Lange's handbook of chemistry*, McGraw-Hill, New Yourk, USA (2005).
36. X.H.,Yu, G. Xie , R.X. Li ,Y.G. Li and Y. Lu, *Sci. China Chem.*,53 (2010) 677.
37. M.J. Barmi and A.N. Nikoloski, *Hydrometallurgy*, 59–66 (2012) 129.
38. U.S. Mohanty, B.C. Tripathy, P. Singh and S.C. Das, *Electroanal. Chem.*, 566 (2004) 47.
39. U.S. Mohanty， B.C. Tripathy， P. Singh and S.C. Das, *J. Appl. Electrochem.*, 31 (2001) 969.
40. M.A. M. Ibrahim and R. Bakdash, *T. I .Met. Finish*, 92 (2014) 218.
41. M. A. M. Ibrahim, *J. Chem. Technol. Biotechnol.*, 75 (2000) 745.
42. Q.B. Zhang and Y.X. Hua, *Mater. Chem. Phys.*, 134 (2012) 333.
43. B.C. Tripathy, S.C. Das and V.N. Misra, *Hydrometallurgy*, 69 (2003) 81.
44. U.S. Mohanty, B.C. Tripathy , S.C. Das , P. Singh and V.N. Misra, *Hydrometallurgy*, 100 (2009) 60.
45. K. Inoue, *Mater. Trans.*, 43 (2002) 1318.
46. R. Winand, *Electrochim. Acta*, 39 (1994) 1091.
47. L. Kumari, S.J. Lin, J.H. Lin, Y.R. Ma, P.C. Lee and Y. Liou, *Appl. Surf. Sci.*, 253 (2007) 5931.
48. U.S. Mohanty, B.C. Tripathy, P. Singh and S.C. Das, *J. Electroanal. Chem.*, 526 (2002) 63.